

## A PDF DESCRIPTION OF TURBULENT PLANE COUETTE FLOW

ZUU-CHANG HONG†, CHING LIN‡ AND MING-HUA CHEN†

†Department of Mechanical Engineering, National Central University, Chungli, Taiwan, R.O.C.

‡Chung-Shan Institute of Science and Technology, Taoyuan, Taiwan, R.O.C.

### ABSTRACT

A transport equation for the one-point velocity probability density function (pdf) of turbulence is derived, modelled and solved. The new pdf equation is obtained by two modeling steps. In the first step, a dynamic equation for the fluid elements is proposed in terms of the fluctuating part of Navier-Stokes equation. A transition probability density function (tpdf) is extracted from the modelled dynamic equation. Then the pdf equation of Fokker-Planck type is obtained from the tpdf. In the second step, the Fokker-Planck type pdf equation is modified by Lundgren's formal pdf equation to ensure it can properly describe the turbulence intrinsic mechanism. With the new pdf equation, the turbulent plane Couette flow is solved by the direct finite difference method coupled with dimensionality reduction and *QUICKER* scheme. A simple boundary treatment is proposed such that the near-wall solution is tractable and then no refined grid is required. The calculated mean velocity, friction coefficient, and turbulence structure are in good agreement with available experimental data. In the region departed from the center of flow field, the contours of isojoint pdf of  $V_1$  and  $V_2$  is very similar to that of experimental result of channel flow. These agreements show the validity of the new pdf model and the availability of the boundary treatment and *QUICKER* scheme for solving the turbulent plane Couette flow.

KEY WORDS Probability density function Transport equation Turbulent flows Couette flow

### INTRODUCTION

Most of the real turbulent shear flows can not be analyzed by the classical statistical turbulence theories due to the extreme complexity of the theories. Therefore, the studies on these problems are almost invoked to the phenomeno-logical theories such as one- or two-equation turbulence models. However, these models deal with only finite order correlation functions and thus many important statistics of turbulence fields can not be described completely.

The similarities between the statistical behaviours of the velocity fluctuations of fluid elements in turbulence fields and those of molecules in a gas kinetic fields suggest the possibility of describing turbulence fields in terms of velocity probability density functions (pdf). The turbulence pdf methods intend to close a system rather than to close some finite moment equations. It provides a way to overcome the shortcomings of classical statistical turbulence theories and phenomenological turbulence models.

Using Hopf's functional formulation<sup>2</sup> and Navier-Stokes equation, Monin<sup>1</sup> first derived a hierarchy of unclosed equations for  $n$ -point probability density function. At the same time, the  $n$ -point pdf equation was also derived by Lundgren<sup>3</sup> using a more efficient method which produces the pdf equation directly from the Navier-Stokes equations. Subsequently, Lundgren<sup>4</sup> employed a Krook model to close the one-point pdf equation and applied it to solve several idealized problems. His model results has shown that the initial shape of the pdf was preserved

0961-5539/95/090757-23\$2.00  
© 1995 Pineridge Press Ltd

Received September 1993  
Revised May 1994

until the turbulence died out and, therefore, no relaxation was achieved. In 1981, Pope<sup>5</sup> employed a pressure-strain closure technique and the Curl's model to close the one-point pdf equation. Although Pope's model contains pressure redistribution and relaxation effects, his model results would produce unrealistic shapes for the probability density function and not lead to a Gaussian as a limit of decaying fluctuations.

Chung<sup>6</sup> proposed his pdf model via a different way. Starting from a generalized Langevin equation, he constructed the transition probability density function of a fluid element in turbulence fields. With the transition probability density function, he obtained a Fokker-Planck type pdf equation. Haworth and Pope<sup>7,8</sup> employed a more generalized Langevin equation<sup>9</sup> to construct their generalized Langevin model. The major difference between Haworth and Pope's model and Chung's model is that there is a more flexible second order tensor  $G_{ij}$  in Haworth and Pope's model than a scalar  $\beta$  in Chung's model. With different choices of  $G_{ij}$ , the Haworth and Pope model can deduce a Reynolds-stress equation to fit specific requirement on the Reynolds-stress model. Bywater<sup>10</sup> and Hong and Lin<sup>11</sup> extended Chung's model for two or more significant degrees of freedom. Their results are too complicated to be applied to real turbulent flow problems. The most serious criticism on the pdf models derived from Langevin type equations is how the Langevin type equation can be used to describe turbulent flows.

A new pdf model of turbulent flows was proposed by the present authors<sup>12,13</sup>. This pdf model was obtained by combining the two methods mentioned above to retain their advantages and avoid their shortcomings. It follows that this new pdf model can describe the statistical behaviour of turbulence fields more properly than the other models.

Due to the highly dimensional characteristics of a probability density function, only a few turbulent flow problems were analyzed by the pdf method<sup>8,14-18</sup>. For the pdf of the velocity field,  $f(X_i, V_i)$  is a function of six independent variables. It is intractable to obtain the solution of a partial differential equation associated with six independent variables by a conventional numerical method such as the finite difference methods or the finite element methods. Moreover, the near-wall treatment is also difficult for the application of a pdf model. Numerical methods employed for solving pdf model with a solid-wall boundary can be only found in the works of Chung<sup>14</sup> and Srinivasan *et al.*<sup>15</sup>. Srinivasan *et al.* used the pdf model proposed by Lundgren<sup>4</sup> to analyze the turbulent plane Couette flow under two types of boundary conditions. But the near-wall Reynolds-stress was overpredicted so that the Reynolds-stress profile was incorrect.

In this paper, the modelling steps in the new pdf will be briefly described. Subsequently, this new pdf equation is solved for the turbulent plane Couette flow. A simple boundary treatment is used to obtain a reasonable near-wall solution without refined grids. Numerical results are obtained by the finite difference method with a *QUICKER* scheme<sup>19</sup>. In the present study, the mean velocity, turbulent energy, Reynolds-stress profiles, and friction coefficient will be examined. These results will be compared with the available experimental data of Reichardt<sup>20</sup>, Robertson *et al.*<sup>21</sup>, and El Telbany *et al.*<sup>22</sup>.

## STOCHASTIC MODEL

This section will briefly describe the derivation of the pdf model. The modelling procedure was divided into two steps.

### *First modelling step*

The dynamic equation governing the fluctuating momentum of fluid elements can be obtained by subtracting Reynolds average equation from Navier-Stokes equation as:

$$\frac{\partial U_i}{\partial t} + \frac{\partial(\langle u_j \rangle U_i)}{\partial X_j} + \frac{\partial(U_j U_i)}{\partial X_j} = -\frac{\partial \langle u_i \rangle}{\partial X_j} U_j + \frac{\partial \langle U_i U_j \rangle}{\partial X_j} - \frac{1}{\rho} \frac{\partial P}{\partial X_i} + \nu \frac{\partial^2 U_i}{\partial X_j \partial X_j} \quad (1)$$

or

$$\frac{dU_i}{dt} = -\frac{\partial \langle u_i \rangle}{\partial X_j} U_j + \frac{\partial \langle U_i U_j \rangle}{\partial X_j} - \frac{1}{\rho} \frac{\partial P}{\partial X_i} + \nu \frac{\partial^2 U_i}{\partial X_j \partial X_j} \tag{2}$$

where  $u_i$  stands for the instantaneous velocity,  $U_i$  for the fluctuating component of velocity  $u_i$ ,  $P$  for the fluctuation of static pressure,  $\rho$  and  $\nu$  for density and kinematic viscosity, respectively,

$\langle \rangle$  represents ensemble mean.  $\frac{d}{dt} = \frac{\partial}{\partial t} + u_i \frac{\partial}{\partial X_i}$  is the material derivative along the path of fluid

elements. The last two terms in the right-hand side of (2) represent the pressure force and viscous force acting on the fluid elements, respectively. These two terms are mainly contributed from the small eddies (high frequency). If one does not want to go into the details of the dynamics of the smallest eddies, the only thing one can say about the smallest eddies is that they are very numerous and very irregular as to their strength and direction. Then the turbulent flows should be treated as a stochastic process and the pressure force and viscous force terms in (2) should be reformulated. In modelling the viscous effect and pressure fluctuation effect, the following assumptions were made:

- 1 The stochastic fluctuations of momentum of fluid elements in turbulence fields is a Markov process.
- 2 For the stochastic process of the high Reynolds number turbulence flows, the viscous force acting on the fluid elements is assumed in proportion to  $-\bar{U}_i/\tau_i$ ,  $\tau_i$  is the characteristic time of the turbulent flow and is assumed in proportion to  $k/\varepsilon$ .  $k$  and  $\varepsilon$  are the turbulent kinetic energy and its dissipation rate, respectively.
- 3 The local fluctuating pressure acting on a fluid element can be treated as the sum of many small pressure forces. For high Reynolds number flows, the fluctuation of momentum due to the pressure force can be simulated as a Wiener process with a Gaussian distribution.

According to (2) and assumptions 2 and 3, in an infinitesimal time interval  $dt$ , the dynamic equations for the change of momentum fluctuations of fluid elements are proposed as:

$$dU_i = \left( -U_j \frac{\partial \langle u_i \rangle}{\partial X_j} + \frac{\partial \langle U_i U_j \rangle}{\partial X_j} + A(t) - C_{f1} \frac{\varepsilon}{k} U_i \right) dt, \tag{3}$$

where  $A(t)$  represents a Wiener process with Gaussian distribution.

From assumption 1, there exists a transition probability density function  $Tr(t, X, V)$  connecting two neighbouring points in the velocity sample-space  $V$ . The stochastic process is completely defined by this transition probability density function. Let  $f(t, X, V)$  be the Eulerian probability density function of the velocity fluctuations in turbulence fields. Then  $f(t, X, V) dV$  is the probability of a fluid element falling between  $(t, X, V)$  and  $(t, X, V + dV)$  in the phase space.  $f(t + dt, X + dX, V)$  can be related to  $f(t, X, V - dV)$  by means of the transition probability density function  $Tr$  in the following way:

$$f(t + \Delta t, X + \Delta X, V) = \iiint f(t, X, V - \Delta V) Tr(t, X, V - \Delta V; \Delta V) d\Delta V. \tag{4}$$

The above equation can be transformed into a differential equation by expanding the various function in Taylor series for small value of  $\Delta t$  as:

$$\left[ \frac{\partial f}{\partial t} + (\langle u_i \rangle + V_i) \frac{\partial f}{\partial X_i} \right] \Delta t + O(\Delta t^2) = -\frac{\partial (f \xi^{V_i})}{\partial V_i} + \frac{1}{2} \frac{\partial^2 (f \xi^{V_i V_j})}{\partial V_i \partial V_j} + O(\xi^{V_i V_j V_k}), \tag{5}$$

where  $\xi^{V_i}$ ,  $\xi^{V_i V_j}$  and  $\xi^{V_i V_j V_k}$  are the transition moments of the first, second and third orders,

respectively, which are defined as:

$$\xi^{V_i} = \iiint \Delta V_i Tr(t, X, V; \Delta V) d\Delta V \quad (6a)$$

$$\xi^{V_i V_j} = \iiint \Delta V_i \Delta V_j Tr(t, X, V; \Delta V) d\Delta V \quad (6b)$$

$$\xi^{V_i V_j V_k} = \iiint \Delta V_i \Delta V_j \Delta V_k Tr(t, X, V; \Delta V) d\Delta V \quad (6c)$$

Once the transition probability density function is found, the pdf governing equation can be obtained by evaluating the transition moments.

The transition probability density function was extracted from the stochastic solution of (3) as:

$$Tr(t, X, V; \Delta R) = \left( \frac{1}{4\pi q \Delta t} \right)^{3/2} EXP \left[ - \left( \frac{\Delta R_1^2}{4q \Delta t} + \frac{\Delta R_2^2}{4q \Delta t} + \frac{\Delta R_3^2}{4q \Delta t} \right) \right] \quad (7)$$

where,

$$\begin{aligned} \Delta R_i &= \Delta V_i - C_i \Delta t + O(\Delta t^2), \\ C_i &= -U_j \frac{\partial \langle u_i \rangle}{\partial X_j} + \frac{\partial \langle U_i U_j \rangle}{\partial X_j} - C_{f1} \frac{\varepsilon}{k} U_i \end{aligned}$$

Then the transition moments can easily be obtained as:

$$\begin{aligned} \xi^{V_i} &= \iiint \Delta V_i Tr(t, X, V; \Delta V) d\Delta V \\ &= C_i \Delta t + O(\Delta t^2) \\ &= \left[ -U_j \frac{\partial \langle u_i \rangle}{\partial X_j} + \frac{\partial \langle U_i U_j \rangle}{\partial X_j} - C_{f1} \frac{\varepsilon}{k} U_i \right] \Delta t + O(\Delta t^2), \end{aligned} \quad (8)$$

$$\begin{aligned} \xi^{V_i V_j} &= \iiint \Delta V_i \Delta V_j Tr(t, X, V; \Delta V) d\Delta V \\ &= \begin{cases} 0 + O(\Delta t^2) & \text{for } i \neq j \\ 2q \Delta t + O(\Delta t^2) & \text{for } i = j \end{cases} \end{aligned} \quad (9)$$

Substituting (8) and (9) into (5), the pdf governing equation for the first step modelling was obtained as:

$$\frac{\partial f}{\partial t} + (\langle u_i \rangle + V_i) \frac{\partial f}{\partial X_i} = \frac{\partial}{\partial V_i} \left[ \left( \frac{\partial \langle u_i \rangle}{\partial X_j} U_j + C_{f1} \frac{\varepsilon}{k} U_i - \frac{\partial \langle U_i U_j \rangle}{\partial X_j} \right) f \right] + \frac{\partial^2 (qf)}{\partial V_i \partial V_i} \quad (10)$$

where  $q$  is an undefined quantity generated from the transition moments.

The Kolmogorov's hypothesis of local isotropy<sup>23</sup> states that if the turbulence is locally isotropic one can express the following relation by properly choosing the time scale  $\tau$ ,

$$\overline{\Delta U_i \Delta U_j} = C_0 \varepsilon \tau \delta_{ij} \quad \text{for } \tau_\eta \ll \tau \ll T_0 \quad (11)$$

where  $\Delta U = U(t)$ ,  $\tau_\eta$  is the Kolmogorov's time scale,  $T_0$  is the characteristic time scale of mean turbulence fields, and  $C_0$  is a universal constant.

In deriving the transition probability density function, the time interval was carefully chosen to fall between the scales of small eddies and large eddies. Therefore the time interval chosen should be of the same range as that in Kolmogorov's locally isotropic turbulence hypothesis

(Eq. (11)). Then one can expect that,

$$\xi^{V_i V_j} \propto \overline{\Delta U_i \Delta U_j}$$

or

$$q = C_{f2} \varepsilon \tag{12}$$

By substituting (12) into (10), a Fokker-Planck type pdf equation gives:

$$\frac{\partial f}{\partial t} + (\langle u_i \rangle + V_i) \frac{\partial f}{\partial X_i} = \frac{\partial}{\partial V_i} \left[ \left( \frac{\partial \langle u_i \rangle}{\partial X_j} U_j + C_{f1} \frac{\varepsilon}{k} U_i - \frac{\partial \langle U_i U_j \rangle}{\partial X_j} \right) f \right] + C_{f2} \frac{\partial^2 f}{\partial V_i \partial V_j} \varepsilon \tag{13}$$

There are two unknown constants,  $C_{f1}$  and  $C_{f2}$ , to be determined. To keep the correct energy dissipation rate in turbulent energy equation deduced from (13), one has:

$$C_{f2} = \frac{(2C_{f1} - 1)}{3} \tag{14}$$

*Second modelling step*

The stochastic model for velocity, (13), proposed by the first modelling step based on the assumptions 2 and 3 would render some turbulence characteristics lost. Therefore, in the second modeling step the formal pdf equation was employed to correct (13) to ensure that the final pdf model could contain the statistic information of turbulence fields more properly.

The associated Reynolds-stress equation derived from the (13) are:

$$\begin{aligned} \frac{\partial \langle U_m U_n \rangle}{\partial t} + \langle u_k \rangle \frac{\partial \langle U_m U_n \rangle}{\partial X_k} + \frac{\partial \langle U_k U_m U_n \rangle}{\partial X_k} = & - \langle U_k U_n \rangle \frac{\partial \langle u_m \rangle}{\partial X_k} - \langle U_k U_m \rangle \frac{\partial \langle u_n \rangle}{\partial X_k} \\ & - 2C_{f1} \frac{\varepsilon}{k} \langle U_m U_n \rangle + 2C_{f2} \delta_{mn} \varepsilon \end{aligned} \tag{15}$$

Comparing (15) with the Reynolds-stress equation derived from Navier-Stokes equations (the pressure diffusion term and viscous work term in the Reynolds-stress equation are neglected), one obtained

$$v \left\langle \frac{\partial U_m}{\partial X_n} \frac{\partial U_n}{\partial X_m} \right\rangle = \begin{cases} 0 & \text{for } m \neq n, \\ \varepsilon/3 & \text{for } m = n, \end{cases} \tag{16a}$$

$$R_{mn} = 2C_{f1} \frac{\varepsilon}{k} \left( \langle U_m U_n \rangle - \frac{2}{3} \delta_{mn} k \right) \tag{16b}$$

where  $R_{mn}$  is the pressure distribution term of Reynolds-stress equation. Equation (16b) is of the same form as the free interaction part of pressure distribution model proposed by Rotta<sup>24</sup> which is accepted by many investigators<sup>25-29</sup>. This implied the isotropic dissipation of small eddies and means that the assumed Wiener process of the pressure fluctuation effects on fluid elements only retains the free interaction part. In general, the mean strain rate vary slowly in flow fields and will produce a non-Gaussian distribution for the acting process of pressure force. Consequently, the forced interaction part of pressure should be added back to the pdf equation, (3).

The assumption 2 of the previous subsection implies that the dissipation rate of turbulence fields is controlled by larger eddies. However, close to the wall the viscous effects become important. Accordingly, an additional term should be added to (3) to take care of the viscous effects.

From the above analysis, a term,  $MP$ , representing the forced interaction effects of pressure

force and a term,  $MV$ , representing the viscous effects were added to (3) as:

$$\frac{\partial U_i}{\partial t} = -U_j \frac{\partial \langle u_i \rangle}{\partial X_j} + \frac{\partial \langle U_i U_j \rangle}{\partial X_j} - C_{f1} \frac{\varepsilon}{k} U_i + A(t) + MP + MV \quad (17)$$

Owing to the additional terms in (17), the pdf equation derived from (17) will contain extra terms other than those in (13). Let's denote these terms as  $MPF$  and  $MVF$  corresponding to the effects of  $MP$  and  $MV$ , respectively. Thus the modified pdf equation can be expressed as:

$$\frac{\partial f}{\partial t} + (\langle u_i \rangle + V_i) \frac{\partial f}{\partial V_i} \left[ \left( \frac{\partial \langle u_i \rangle}{\partial X_j} U_j + C_{f1} \frac{\varepsilon}{k} U_i - \frac{\partial \langle U_i U_j \rangle}{\partial X_j} \right) f \right] + C_{f2} \frac{\partial^2 f}{\partial V_i \partial V_j} \varepsilon + MPF + MVF \quad (18)$$

Comparing with the Lundgren's pdf equation, one tries to identify the  $MPF$  and  $MVF$  in (18). The Lundgren's pdf equation is:

$$\frac{\partial f}{\partial t} + (\langle u_i \rangle + V_i) \frac{\partial f}{\partial X_i} = \frac{\partial}{\partial V_i} \left[ \left( \frac{\partial \langle u_i \rangle}{\partial X_j} U_j - \frac{\partial \langle U_i U_j \rangle}{\partial X_j} \right) f \right] + \frac{1}{\rho} \left\langle \frac{\partial \tilde{f}}{\partial V_i} \frac{\partial P}{\partial X_i} \right\rangle - \left\langle v \frac{\partial^2 U_i}{\partial X_j \partial X_j} \frac{\partial \tilde{f}}{\partial V_i} \right\rangle \quad (19)$$

or

$$\begin{aligned} \frac{\partial f}{\partial t} + (\langle u_i \rangle + V_i) \frac{\partial f}{\partial X_i} = \frac{\partial}{\partial V_i} \left[ \left( \frac{\partial \langle u_i \rangle}{\partial X_j} U_j - \frac{\partial \langle U_i U_j \rangle}{\partial X_j} \right) f \right] + \frac{1}{\rho} \frac{\partial^2 \langle \tilde{f} P \rangle}{\partial X_i \partial V_i} \\ + \frac{1}{\rho} \frac{\partial^2 \langle \tilde{f} P \frac{\partial U_j}{\partial X_i} \rangle}{\partial V_i \partial V_j} + v \frac{\partial^2 f}{\partial X_j \partial X_j} - \left\langle v \frac{\partial U_i}{\partial X_j} \frac{\partial U_k}{\partial X_j} \frac{\partial^2 \tilde{f}}{\partial V_k \partial V_i} \right\rangle \end{aligned} \quad (20)$$

where  $\tilde{f}$  is the fine-grained density which is defined as:

$$\begin{aligned} \tilde{f} &\equiv \delta(U(t, X) - V) \\ &= \tilde{f}(t, X; V) \end{aligned} \quad (21)$$

and the ensemble average of the fine-grained density is the pdf  $f$ , i.e.,

$$f \equiv \langle \tilde{f} \rangle. \quad (22)$$

The last four terms in the right-hand side of (20) are obtained from the two unclosed terms in (19) which are due to the effects of the pressure and viscous forces, respectively. The first term involved derivatives with respect to  $X_i$  and  $V_i$  indicates the pressure diffusion transport. The second term involved derivative with respect to  $V_i$  only denotes the pressure redistribution of  $f$  in  $V$  space. The third term is the molecular transport of  $f$  in  $V$  space. The last term,  $\left\langle v \frac{\partial U_i}{\partial X_j} \frac{\partial U_k}{\partial X_j} \frac{\partial^2 \tilde{f}}{\partial V_k \partial V_i} \right\rangle$ , would result in viscous dissipation,  $\left\langle v \frac{\partial U_i}{\partial X_k} \frac{\partial U_j}{\partial X_k} \right\rangle$ , which can be obtained from being multiplied by  $U_i U_j$  and integrated over  $V$  space.

It is obvious that  $MVF$  and  $MPF$  are related to the last four terms of (20). From the previous analysis the pdf transport equation obtained by the first modelling step keeps the effect of the last term of (20) under the condition of isotropic dissipation. In the present analysis, we let

$MVF = v \frac{\partial^2 f}{\partial X_k \partial X_k}$  take care of the molecular viscous effect on the transport of  $f$  which is

significant in the near wall region. As mentioned previously, the Wiener process maintains the free interaction effect of pressure diffusion only, the term  $MPF$  should contain three parts,

$$\frac{1}{\rho} \frac{\partial^2 \langle \tilde{f} P_1 \rangle}{\partial X_i \partial V_i}, \quad \frac{1}{\rho} \frac{\partial^2 \langle \tilde{f} P_2 \rangle}{\partial X_i \partial V_i}, \quad \text{and} \quad \frac{1}{\rho} \frac{\partial^2 \langle \tilde{f} P_1 \frac{\partial U_j}{\partial X_i} \rangle}{\partial V_i \partial V_j}$$

which denote the forced and free interaction of pressure diffusion term and the forced interaction of pressure redistribution term, respectively.

To consider the pressure redistribution effect only and refer to the original form of the pressure redistribution terms, *MPF* was proposed as

$$MPF = \frac{\partial \langle u_k \rangle}{\partial X_i} \frac{\partial^2 (C_{pqijkl}^1 \langle U_p U_q \rangle f)}{\partial V_i \partial V_j} + \frac{\partial \langle u_i \rangle}{\partial X_m} \frac{\partial (C_{qmti}^2 U_q f)}{\partial V_i} \tag{23}$$

where  $C_{pqijkl}^1$  and  $C_{qmti}^2$  are the dimensionless six- and four-order tensors, respectively. Equation (23) shows that it contains both large and small eddy effects to simulate the pressure redistribution effects.

The pressure redistribution term of Reynolds stress equation has been modelled by many investigators<sup>25-29</sup>. These models can be employed to evaluate  $C_{pqijkl}^1$  and  $C_{qmti}^2$ . The present analysis adopted the Naot *et al.*'s<sup>28</sup> and the Reynolds<sup>29</sup> models of the forced interaction part of pressure redistribution term which was given as:

$$R_{mn}^{(1)} = C_p \left[ \frac{\partial \langle u_n \rangle}{\partial X_i} \langle U_m U_i \rangle + \frac{\partial \langle u_m \rangle}{\partial X_i} \langle U_n U_i \rangle - \frac{2}{3} \delta_{nm} \frac{\partial \langle u_j \rangle}{\partial X_j} \langle U_j U_i \rangle \right] \tag{24}$$

The  $R_{mn}^{(1)}$  derived from (23) is:

$$R_{mn}^{(1)} = C_{pqijkl}^1 \frac{\partial \langle u_k \rangle}{\partial X_i} \langle U_p U_q \rangle (\delta_{mi} \delta_{nj} + \delta_{ni} \delta_{mj}) - C_{qitj}^2 \frac{\partial \langle u_i \rangle}{\partial X_i} (\delta_{ni} \langle U_m U_q \rangle + \delta_{nj} \langle U_m U_q \rangle) \tag{25}$$

By comparing (24) with (25), the simplest choice of  $C_{pqijkl}^1$  and  $C_{qitj}^2$  is:

$$C_{pqijkl}^1 = -\frac{1}{3} C_p \delta_{ij} \delta_{kp} \delta_{lq} \tag{26}$$

$$C_{qitj}^2 = -C_p \delta_{iq} \delta_{lj} \tag{27}$$

The final pdf equation becomes:

$$\begin{aligned} \frac{\partial f}{\partial t} + (\langle u_i \rangle + V_i) \frac{\partial f}{\partial X_i} = & \frac{\partial}{\partial V_i} \left[ (1 - C_p) \frac{\partial \langle u_i \rangle}{\partial X_j} U_j f + C_{f1} \frac{\varepsilon}{k} U_i f - \frac{\partial \langle U_i U_j \rangle}{\partial X_j} f \right] \\ & + \nu \frac{\partial^2 f}{\partial X_i \partial X_i} + \left( C_{f2} \varepsilon - \frac{C_p}{3} \frac{\partial \langle u_m \rangle}{\partial X_n} \langle U_m U_n \rangle \right) \frac{\partial^2 f}{\partial V_i \partial V_i} \end{aligned} \tag{28}$$

Since  $-\frac{\partial \langle u_m \rangle}{\partial X_n} \cdot \langle U_m U_n \rangle$  in (28) is the same as the turbulent energy production term in the turbulent kinetic energy equation, it is positive in most regions of flow fields. If it becomes negative, its magnitude is small in general. We expect that  $C_{f2} \varepsilon - \frac{C_p}{3} \frac{\partial \langle u_m \rangle}{\partial X_n} \cdot \langle U_m U_n \rangle$  would keep positive. In the model of Naot *et al.*<sup>28</sup> the value of  $C_p$  ranged from 0.4 to 0.6. In order to ensure that no negative diffusivity occurs, the value of  $C_p$  is evaluated as follows,

$$C_p = \begin{cases} \frac{-3C_{f2}\varepsilon}{Prod} & \text{for } Prod < 0 \text{ and } \frac{-3C_{f2}\varepsilon}{Prod} < \alpha \\ \alpha & \text{otherwise,} \end{cases}$$

where  $\alpha = 0.4 \sim 0.6$  and

$$Prod = -\frac{\partial \langle u_m \rangle}{\partial X_n} \langle U_m U_n \rangle \tag{29}$$

The constant  $C_{f1}$  can also be determined from the Rotta's model as:

$$C_{f1} = 0.75 \quad (30)$$

The  $C_{f2}$  can be determined from (14) as:

$$C_{f2} = \frac{(2C_{f1} - 1)}{3} = \frac{1}{6}$$

#### pdf EQUATION FOR TURBULENT PLANE COUETTE FLOW

Subsequently, a steady, incompressible turbulent plane Couette flow is solved by the new model derived above. The terms involved in  $\partial/\partial t$ ,  $\partial/\partial X_1$ ,  $\partial/\partial X_3$  are zero, and  $\langle u_2 \rangle$  and  $\langle u_3 \rangle$  are also zero. Thus (28) becomes,

$$\begin{aligned} V_2 \frac{\partial f}{\partial X_2} = & (1 - C_p) \frac{\partial \langle u_1 \rangle}{\partial X_2} \frac{\partial (U_2 f)}{\partial V_1} - \frac{\partial \langle U_1 U_2 \rangle}{\partial X_2} \frac{\partial f}{\partial V_1} + C_{f1} \frac{\varepsilon}{k} \frac{\partial (U_i f)}{\partial V_i} \\ & + \nu \frac{\partial^2 f}{\partial X_2 \partial X_2} + \left( C_{f2} \varepsilon - \frac{C_p}{3} \frac{\partial \langle u_1 \rangle}{\partial X_2} \langle U_1 U_2 \rangle \right) \frac{\partial^2 f}{\partial V_i \partial V_i} \end{aligned} \quad (32)$$

The distribution function  $f$  in (32) is four dimensionality. It is necessary to reduce the dimensionality of  $f$  for computer storage requirement. In Couette flow,  $\langle U_1 U_2 \rangle$  decides the mean velocity profile and the probability distribution of  $V_3$  is less important than that of  $V_1$  and  $V_2$ . Thus (32) can be reduced to three-dimensionality by introducing a set of reduced distribution function as:

$$g(X_2, V_1, V_2) = \int f(X_2, V_1, V_2, V_3) dV_3 \quad (33a)$$

$$h(X_2, V_1, V_2) = \int V_3 f(X_2, V_1, V_2, V_3) dV_3 \quad (33b)$$

$$j(X_2, V_1, V_2) = \int V_3 V_3 f(X_2, V_1, V_2, V_3) dV_3 \quad (33c)$$

By definition these distribution functions should satisfy the following constraints:

$$\iint g(X_2, V_1, V_2) dV_1 dV_2 = 1 \quad (34a)$$

$$\iint h(X_2, V_1, V_2) dV_1 dV_2 = 0 \quad (34b)$$

$$\iint V_1 g(X_2, V_1, V_2) dV_1 dV_2 = 0 \quad (34c)$$

$$\iint V_2 g(X_2, V_1, V_2) dV_1 dV_2 = 0 \quad (34d)$$

The (34a) indicates that the total probability of finding a fluid element somewhere in  $X$ , over the whole  $V$  space is unity, while (34c), and (34d) represent that the mean of fluctuating components of velocity should be zero.



It is convenient to define the following dimensionless variables,

$$\begin{aligned} \tilde{X}_2 &= X_2/H, & \tilde{V}_1 &= V_1/\langle u_1 \rangle_c, & \tilde{V}_2 &= V_2/\langle u_1 \rangle_c, & \tilde{u}_1 &= u_1/\langle u_1 \rangle_c \\ \tilde{g} &= \langle u_1 \rangle_c^2 g, & \tilde{h} &= \langle u_1 \rangle_c h, & \tilde{j} &= j, & \tilde{p} &= p/(\rho \langle u_1 \rangle_c^2) \\ \langle \tilde{U}_i \tilde{U}_j \rangle &= \langle U_i U_j \rangle / \langle u_1 \rangle_c^2, & \tilde{k} &= k / \langle u_1 \rangle_c^2, & \tilde{\varepsilon} &= \varepsilon H / \langle u_1 \rangle_c^3 \\ & & Re &= \langle u_1 \rangle_c H / \nu \end{aligned}$$

where  $\langle u_1 \rangle_c$  is the average velocity of the upper and lower plates, and  $2H$  is the width of the two plates.

The final form of distribution function equations can be rewritten as (for convenience, the accents ( $\tilde{\phantom{x}}$ ) will be dropped from the dimensionless equations):

$$\begin{aligned} V_2 \frac{\partial g}{\partial X_2} &= (1 - C_p) \frac{\partial \langle u_1 \rangle}{\partial X_2} \frac{\partial (U_2 g)}{\partial V_1} - \frac{\partial \langle U_1 U_2 \rangle}{\partial X_2} \frac{\partial g}{\partial V_1} - \frac{\partial \langle U_2 U_2 \rangle}{\partial X_2} \frac{\partial g}{\partial V_2} \\ &+ \left( C_{f2} \varepsilon - \frac{C_p}{3} \frac{\partial \langle u_1 \rangle}{\partial X_2} \langle U_1 U_2 \rangle \right) \left( \frac{\partial^2 g}{\partial V_1 \partial V_1} + \frac{\partial^2 g}{\partial V_2 \partial V_2} \right) + \frac{1}{R_e} \frac{\partial^2 g}{\partial X_2 \partial X_2} \\ &+ C_{f1} \frac{\varepsilon}{k} \left[ \frac{\partial (U_1 g)}{\partial V_1} + \frac{\partial (U_2 g)}{\partial V_2} \right] \end{aligned} \tag{35}$$

$$\begin{aligned} V_2 \frac{\partial h}{\partial X_2} &= (1 - C_p) \frac{\partial \langle u_1 \rangle}{\partial X_2} \frac{\partial (U_2 h)}{\partial V_1} - \frac{\partial \langle U_1 U_2 \rangle}{\partial X_2} \frac{\partial h}{\partial V_1} - \frac{\partial \langle U_2 U_2 \rangle}{\partial X_2} \frac{\partial h}{\partial V_2} \\ &+ \frac{\partial \langle U_2 U_3 \rangle}{\partial X_2} g + \frac{1}{R_e} \frac{\partial^2 h}{\partial X_2 \partial X_2} + C_{f1} \frac{\varepsilon}{k} \left[ \frac{\partial (U_1 h)}{\partial V_1} + \frac{\partial (U_2 h)}{\partial V_2} \right] \\ &+ \left( C_{f2} \varepsilon - \frac{C_p}{3} \frac{\partial \langle u_1 \rangle}{\partial X_2} \langle U_1 U_2 \rangle \right) \left( \frac{\partial^2 h}{\partial V_1 \partial V_1} + \frac{\partial^2 h}{\partial V_2 \partial V_2} \right) \end{aligned} \tag{36}$$

$$\begin{aligned} V_2 \frac{\partial j}{\partial X_2} &= (1 - C_p) \frac{\partial \langle u_1 \rangle}{\partial X_2} \frac{\partial (U_2 j)}{\partial V_1} - \frac{\partial \langle U_1 U_2 \rangle}{\partial X_2} \frac{\partial j}{\partial V_1} - \frac{\partial \langle U_2 U_2 \rangle}{\partial X_2} \frac{\partial j}{\partial V_2} \\ &+ 2 \frac{\partial \langle U_2 U_3 \rangle}{\partial X_2} h - 2 C_{f1} \frac{\varepsilon}{k} j + \frac{1}{R_e} \frac{\partial^2 j}{\partial X_2 \partial X_2} + C_{f1} \frac{\varepsilon}{k} \left[ \frac{\partial (U_1 j)}{\partial V_1} + \frac{\partial (U_2 j)}{\partial V_2} \right] \\ &+ \left( C_{f2} \varepsilon - \frac{C_p}{3} \frac{\partial \langle u_1 \rangle}{\partial X_2} \langle U_1 U_2 \rangle \right) \left( \frac{\partial^2 j}{\partial V_1 \partial V_1} + \frac{\partial^2 j}{\partial V_2 \partial V_2} + 2g \right) \end{aligned} \tag{37}$$

Having Equations (35), (36), and (37) one must employ a mean velocity equation and turbulent energy dissipation rate equation for a self-contained system. For turbulent plane Couette flow, the dimensionless equations of mean velocity and dissipation rate are:

$$\frac{dP}{dX_1} + \frac{d \langle U_1 U_2 \rangle}{dX_2} = \frac{1}{R_e} \frac{d^2 \langle u_1 \rangle}{dX_2^2}, \tag{38}$$

$$C_\varepsilon \frac{d}{dX_2} \left( \frac{k}{\varepsilon} \langle U_2 U_2 \rangle \frac{d\varepsilon}{dX_2} \right) = C_{\varepsilon 1} \langle U_1 U_2 \rangle \frac{d \langle u_1 \rangle}{dX_2} \frac{\varepsilon}{k} - C_{\varepsilon 2} \frac{\varepsilon^2}{k}, \tag{39}$$

where  $C_{\varepsilon 1}$ ,  $C_{\varepsilon 2}$  and  $C_\varepsilon$  are 1.44, 1.90 and 0.15, respectively, as suggested by Launder *et al.*<sup>27</sup>

## NEAR-WALL TREATMENTS AND BOUNDARY CONDITIONS

As mentioned previously, close to the wall the validity of the pdf model is the major obstruction in applications of pdf model. In general, the model equations for turbulence were derived under the conditions far from solid wall, whether in pdf modelling or phenomenological turbulence modelling. It is easy to handle this problem by using the phenomenological turbulence models because there are wall functions can be employed for calculations. However, in a pdf model no wall function can be applied. Under this condition we shall propose a feasible way for the applications of the pdf model near a solid wall.

Srinivasan *et al.*<sup>15</sup> used two kinds of methods to find  $f(X, V)$  at near-wall region. They used the zero gradient distribution function method and the Chapman-Enskog distribution function method to calculate pdf at the near-wall region where the Reynolds stress is constant and the turbulent energy is conservative. There are two main characteristics in turbulent plane Couette flow. One is that the Reynolds stress  $\langle U_1 U_2 \rangle$  is a monotonic function in each symmetric flow domain. The minimum value occurs at the center of flow region. The other is that the turbulent energy has a peak value near the wall. The turbulent energy was not presented in Srinivasans' paper<sup>15</sup>. But the Reynolds stress they gave was overpredicted so that there exists a peak value near the wall. In the present paper a pdf model can be applied without confining to a constant shear stress and can be easily extended to more complicated problem.

In order to take wall effects into consideration, one would modify the pdf equation to fit the near-wall conditions. In deriving the pdf model, it was assumed that the fluctuating momentum is proportional to  $C_{f1} U_i \varepsilon / k$ . This implies that each momentum component exhibits the same characteristic relaxation rate. For the near-wall region this condition will be violated. So we assume the fluctuating momentum near the wall is proportional to  $2C_{f1} U_i \varepsilon / 3U_i'^2$  where  $U_i'$  is turbulence intensity defined as:

$$U_i' = \left[ \int V_i^2 f(X_j, V_j) dV_j \right]^{1/2}, \quad (\text{no sum on } i)$$

and the value of  $C_{f1}$  is fixed.

From experimental data of turbulent energy balance<sup>30</sup> one can find that the pressure transport effects neglected in this pdf model is important near the viscous sublayer. This term is of the same order as energy generation term in turbulent energy equation. Because the pressure transport effects are not well modelled, we lump this effect to the term in pdf equation corresponding to turbulent energy generation term of its moment equation by a factor  $C_{1p}$ . Therefore, the governing pdf equation for the nearest wall point can be written as:

$$\begin{aligned} V_2 \frac{\partial f}{\partial X_2} = & (C_{1p} - C_p) \frac{\partial \langle u_1 \rangle}{\partial X_2} \frac{\partial (U_2 f)}{\partial V_1} - \frac{\partial \langle U_1 U_2 \rangle}{\partial X_2} \frac{\partial f}{\partial V_i} + \frac{2C_{f1}}{3} \frac{\varepsilon}{U_i'^2} \frac{\partial (U_i f)}{\partial V_i} \\ & + v \frac{\partial^2 f}{\partial X_2 \partial X_2} + \left( C_{f2} \varepsilon - \frac{C_p}{3} \frac{\partial \langle u_1 \rangle}{\partial X_2} \langle U_1 U_2 \rangle \right) \frac{\partial^2 f}{\partial V_i \partial V_i} \end{aligned} \quad (40)$$

and the corresponding equations for  $g$ ,  $h$ , and  $j$  are,

$$\begin{aligned} V_2 \frac{\partial g}{\partial X_2} = & (C_{1p} - C_p) \frac{\partial \langle u_1 \rangle}{\partial X_2} \frac{\partial (U_2 g)}{\partial V_1} - \frac{\partial \langle U_1 U_2 \rangle}{\partial X_2} \frac{\partial g}{\partial V_1} - \frac{\partial \langle U_2 U_2 \rangle}{\partial X_2} \frac{\partial g}{\partial V_2} \\ & + \left( C_{f2} \varepsilon - \frac{C_p}{3} \frac{\partial \langle u_1 \rangle}{\partial X_2} \langle U_1 U_2 \rangle \right) \left( \frac{\partial^2 g}{\partial V_1 \partial V_1} + \frac{\partial^2 g}{\partial V_2 \partial V_2} \right) \\ & + \frac{2C_{f1} \varepsilon}{3U_1'^2} \frac{\partial (U_1 g)}{\partial V_1} + \frac{2C_{f1} \varepsilon}{3U_2'^2} \frac{\partial (U_2 g)}{\partial V_2} + \frac{1}{R_e} \frac{\partial^2 g}{\partial X_2 \partial X_2} \end{aligned} \quad (41a)$$

$$\begin{aligned}
 V_2 \frac{\partial h}{\partial X_2} = & (C_{1p} - C_p) \frac{\partial \langle u_1 \rangle}{\partial X_2} \frac{\partial (U_2 h)}{\partial V_1} - \frac{\partial \langle U_1 U_2 \rangle}{\partial X_2} \frac{\partial h}{\partial V_1} - \frac{\partial \langle U_2 U_2 \rangle}{\partial X_2} \frac{\partial h}{\partial V_2} \\
 & + \frac{2C_{f1}\epsilon}{3U_1'^2} \frac{\partial (U_1 h)}{\partial V_1} + \frac{2C_{f1}\epsilon}{3U_2'^2} \frac{\partial (U_2 h)}{\partial V_2} + \frac{1}{R_e} \frac{\partial^2 h}{\partial X_2 \partial X_2} + \frac{\partial \langle U_2 U_3 \rangle}{\partial X_2} g \\
 & + \left( C_{f2}\epsilon - \frac{C_p}{3} \frac{\partial \langle u_1 \rangle}{\partial X_2} \langle U_1 U_2 \rangle \right) \left( \frac{\partial^2 h}{\partial V_1 \partial V_1} + \frac{\partial^2 h}{\partial V_2 \partial V_2} \right) \tag{41b}
 \end{aligned}$$

$$\begin{aligned}
 V_2 \frac{\partial j}{\partial X_2} = & (C_{1p} - C_p) \frac{\partial \langle u_1 \rangle}{\partial X_2} \frac{\partial (U_2 j)}{\partial V_1} - \frac{\partial \langle U_1 U_2 \rangle}{\partial X_2} \frac{\partial j}{\partial V_1} - \frac{\partial \langle U_2 U_2 \rangle}{\partial X_2} \frac{\partial j}{\partial V_2} \\
 & + 2 \frac{\partial \langle U_2 U_3 \rangle}{\partial X_2} h + \frac{1}{R_e} \frac{\partial^2 j}{\partial X_2 \partial X_2} + \frac{2C_{f1}\epsilon}{3U_1'^2} \frac{\partial (U_1 j)}{\partial V_1} + \frac{2C_{f1}\epsilon}{\partial V_1} + \frac{2C_{f1}\epsilon}{3U_2'^2} \frac{\partial (U_2 j)}{\partial V_2} - \frac{4C_{f1}\epsilon}{3U_3'^2} j \\
 & + \left( C_{f2}\epsilon - \frac{C_p}{3} \frac{\partial \langle u_1 \rangle}{\partial X_2} \langle U_1 U_2 \rangle \right) \left( \frac{\partial^2 j}{\partial V_1 \partial V_1} + \frac{\partial^2 j}{\partial V_2 \partial V_2} + 2g \right) \tag{41c}
 \end{aligned}$$

where  $C_{1p}$  is chosen as 2.0.

Since the pressure redistribution terms are modelled by the Green function of the pressure equation, one must take the surface integration part solution near the wall region into account. Launder *et al.*<sup>27</sup> have modified the corresponding terms in Reynolds-stress model. We will directly employ the results in the present calculations, i.e.,

$$C_p = 0.6 + 0.015 \frac{k^{3/2}}{\epsilon X_2} \tag{42a}$$

$$C_{f1} = 0.75 + 0.0625 \frac{k^{3/2}}{\epsilon X_2} \tag{42b}$$

The modified model should satisfy the boundary conditions (on the solid wall). For viscous flow, the no-slip condition must hold on the solid wall. One has,

$$f(X_{2w}, V_1, V_2, V_3) = \delta(V_1 - 0) \delta(V_2 - 0) \delta(V_3 - 0) \tag{43a}$$

where  $X_{1w}$  represents the position of the wall. The corresponding boundary conditions for the reduced distribution function are:

$$g(X_{2w}, V_1, V_2) = \delta(V_1 - 0) \delta(V_2 - 0) \tag{43b}$$

$$h(X_{2w}, V_1, V_2) = 0 \tag{43c}$$

$$j(X_{2w}, V_1, V_2) = 0 \tag{43d}$$

Since the mean velocity and turbulent energy dissipation rate are well predicted by using the phenomenological turbulence model, in the present calculations the law for near-wall velocity is adopted and the near-wall dissipation rate is assumed to be equal to the turbulent energy generation rate. Then the boundary conditions for mean velocity and dissipation rate equation are:

$$\langle u_1 \rangle^+ = \begin{cases} \frac{1}{\kappa} \ln(\epsilon X_2^+) & \text{for } X_2^+ > 11.6 \\ X_2^+ & \text{for } X_2^+ < 11.6 \end{cases} \tag{44a}$$

$$\epsilon = -\langle U_1 U_2 \rangle \frac{\partial \langle u_1 \rangle}{\partial X_2} \tag{44b}$$

where  $\kappa$  is the Karmman's constant ( $=0.42$ ),  $E$  is the constant for wall roughness,  $\langle u_1 \rangle^+ = \langle u_1 \rangle / u_\tau$ , and  $X_2^+ = X_2 u_\tau / \nu$ . In this case we chose  $E=9.0$  for smooth wall.

### NUMERICAL METHOD

For the calculation of fluid flow problems, there are a number of numerical methods, such as finite-difference methods<sup>31</sup> or SIMPLE algorithm.<sup>32</sup> Among these methods, the first order upwind and hybrid difference schemes for the first derivative terms are most stable in high Reynolds number flow problems for stability consideration. Although the artificial viscosity will increase the diffusion effect, the turbulence fields will not be severely distorted in the calculations using the phenomenological turbulence model. In the present pdf model, however, the first and the second derivatives in velocity phase space strongly affect the turbulence energy. The artificial viscosity contributed from these derivatives will cause a nonphysical source in the turbulent energy equation. Thus, the high order scheme will be needed to reduce the artificial viscosity. Accordingly, for  $X_2$  space we chose hybrid scheme and for  $V_1$  and  $V_2$  spaces the *QUICKER*<sup>19</sup> scheme (*QUICK* Extended and Revised form), which was obtained by rearranging the *QUICK*<sup>33</sup> scheme to be more stable, is used. For the second derivative terms, the central difference is used.

Equations (35), (36) and (37) can be casted into the general form as follows:

$$\frac{\partial(\tilde{C}^{X_2}\Phi)}{\partial X_2} + \frac{\partial(\tilde{C}^{V_1}\Phi)}{\partial V_1} + \frac{\partial(\tilde{C}^{V_2}\Phi)}{\partial V_2} = \frac{\partial\left(\tilde{D}^{X_2} \frac{\partial\Phi}{\partial X_2}\right)}{\partial X_2} + \frac{\partial\left(\tilde{D}^{V_1} \frac{\partial\Phi}{\partial V_1}\right)}{\partial V_1} + \frac{\partial\left(\tilde{D}^{V_2} \frac{\partial\Phi}{\partial V_2}\right)}{\partial V_2} + S_\Phi \quad (45)$$

where,

$$\tilde{C}^{X_2} = U_2,$$

$$\tilde{C}^{V_1} = \frac{\partial\langle U_1 U_2 \rangle}{\partial X_2} - (1 - C_p) \frac{\partial\langle u_1 \rangle}{\partial X_2} U_2 - C_{f1} \frac{\varepsilon U_1}{k}$$

$$\tilde{C}^{V_2} = \frac{\partial\langle U_2 U_2 \rangle}{\partial X_2} - C_{f1} \frac{\varepsilon U_2}{k}$$

$$\tilde{D}^{X_2} = \frac{1}{Re}$$

$$\tilde{D}^{V_1} = C_{f2} \varepsilon - \frac{C_p}{3} \frac{\partial\langle u_1 \rangle}{\partial X_2} \langle U_1 U_2 \rangle$$

$$\tilde{D}^{V_2} = C_{f2} \varepsilon - \frac{C_p}{3} \frac{\partial\langle u_1 \rangle}{\partial X_2} \langle U_2 U_2 \rangle$$

$\Phi$  denotes the reduced distribution function and  $S_\Phi$  are the source terms of  $\Phi$ -equation defined as:

$$S_g = 0$$

$$S_j = \frac{\partial\langle U_2 U_3 \rangle}{\partial X_2} g$$

$$S_h = 2 \frac{\partial\langle U_2 U_3 \rangle}{\partial X_2} h + 2 \left( C_{f2} \varepsilon - \frac{C_p}{3} \frac{\partial\langle u_1 \rangle}{\partial X_2} \langle U_1 U_2 \rangle \right) g - 2 C_{f1} \frac{\varepsilon}{k} j$$

In general, the finite difference equation for (45) can be written as the following form<sup>19</sup>:

$$\Phi_{x,u,v} = (B_{x+1}^\Phi \Phi_{x+1,u,v} + B_{x-1}^\Phi \Phi_{x-1,u,v} + B_{u+1}^\Phi \Phi_{x,u+1,v} + B_{u-1}^\Phi \Phi_{x,u-1,v} + B_{v+1}^\Phi \Phi_{x,u,v+1} + B_{v-1}^\Phi \Phi_{x,u,v-1} + S_a^\Phi) / (B^\Phi \Phi_{x,u,v} - S_b^\Phi) \quad (46)$$

where  $B_s'$  are the coefficients contributed from the first- and second-derivative terms and  $S_s'$  are the source terms due to transforming the partial differential equations into their finite difference counterparts, not explicitly shown in (46). The subscript index  $x, u$  and  $v$  represent the  $X_2, V_1$  and  $V_2$  coordinates, respectively.

Now, the hybrid and *QUICKER* schemes are used for physical and velocity spaces, respectively. The corresponding  $B_s'$  and  $S_s'$  are:

$$\begin{aligned}
 B_{x+1}^\Phi &= \left[ \left[ 0, (D_{x+1}^{x_2} - 0.5C_{x+1}^{x_2}), -C_{x+1}^{x_2} \right] \right] \\
 B_{x-1}^\Phi &= \left[ \left[ 0, (D_{x-1}^{x_2} + 0.5C_{x-1}^{x_2}), -C_{x-1}^{x_2} \right] \right] \\
 B_{u+1}^\Phi &= \left[ \left[ \left( D_{u+1}^{v_1} + \frac{3}{4}C_{u+1}^{v_1} \right), \left( D_{u+1}^{v_1} - \frac{3}{4}C_{u+1}^{v_1} - \frac{1}{8}C_{u-1}^{v_1} \right), \left( D_{u+1}^{v_1} - \frac{3}{4}C_{u+1}^{v_1} \right), \right. \right. \\
 &\quad \left. \left. \left( D_{u+1}^{v_1} + \frac{3}{4}C_{u+1}^{v_1} - \frac{1}{8}C_{u-1}^{v_1} \right) \right] \right] \\
 B_{u-1}^\Phi &= \left[ \left[ \left( D_{u-1}^{v_1} - \frac{3}{4}C_{u-1}^{v_1} \right), \left( D_{u-1}^{v_1} + \frac{3}{4}C_{u-1}^{v_1} + \frac{1}{8}C_{u+1}^{v_1} \right), \left( D_{u-1}^{v_1} + \frac{3}{4}C_{u-1}^{v_1} \right), \right. \right. \\
 &\quad \left. \left. \left( D_{u-1}^{v_1} - \frac{3}{4}C_{u-1}^{v_1} + \frac{1}{8}C_{u+1}^{v_1} \right) \right] \right] \\
 B_{v+1}^\Phi &= \left[ \left[ \left( D_{v+1}^{v_2} + \frac{3}{4}C_{v+1}^{v_2} \right), \left( D_{v+1}^{v_2} - \frac{3}{4}C_{v+1}^{v_2} - \frac{1}{8}C_{v-1}^{v_2} \right), \left( D_{v+1}^{v_2} - \frac{3}{4}C_{v+1}^{v_2} \right), \right. \right. \\
 &\quad \left. \left. \left( D_{v+1}^{v_2} + \frac{3}{4}C_{v+1}^{v_2} - \frac{1}{8}C_{v-1}^{v_2} \right) \right] \right] \\
 B_{v-1}^\Phi &= \left[ \left[ \left( D_{v-1}^{v_2} - \frac{3}{4}C_{v-1}^{v_2} \right), \left( D_{v-1}^{v_2} + \frac{3}{4}C_{v-1}^{v_2} + \frac{1}{8}C_{v+1}^{v_2} \right), \left( D_{v-1}^{v_2} + \frac{3}{4}C_{v-1}^{v_2} \right), \right. \right. \\
 &\quad \left. \left. \left( D_{v-1}^{v_2} - \frac{3}{4}C_{v-1}^{v_2} + \frac{1}{8}C_{v+1}^{v_2} \right) \right] \right] \\
 B &= B_{x+1}^\Phi + B_{x-1}^\Phi + B_{u+1}^\Phi + B_{u-1}^\Phi + B_{v+1}^\Phi + B_{v-1}^\Phi
 \end{aligned}$$

$$\begin{aligned}
 \tilde{S}^\Phi &= \left[ \frac{1}{8} (M_{u+1}^+ C_{u+1}^{v_1} + M_{v+1}^+ C_{v+1}^{v_2} - M_{u-1}^- C_{u-1}^{v_1} - M_{v-1}^- C_{v-1}^{v_2}) \right. \\
 &\quad \left. + \frac{9}{8} (M_{v+1}^+ C_{v-1}^{v_2} + M_{u-1}^+ C_{u-1}^{v_1} - M_{u+1}^- C_{u+1}^{v_1} - M_{v+1}^- C_{v+1}^{v_2}) \right] \Phi_{x,u,v} \\
 &\quad - \frac{1}{8} [M_{u-1}^+ C_{u-1}^{v_1} \Phi_{x,u-2,v} + M_{v-1}^+ C_{v-1}^{v_2} \Phi_{x,u,v-2} - M_{u+1}^- C_{u+1}^{v_1} \Phi_{x,u+2,v} - M_{v+1}^- C_{v+1}^{v_2} \Phi_{x,u,v+2}] \\
 &\quad - \frac{9}{8} [M_{u+1}^+ C_{u+1}^{v_1} \Phi_{x,u+1,v} + M_{v+1}^+ C_{v+1}^{v_2} \Phi_{x,u,v+1} - M_{u-1}^- C_{u-1}^{v_1} \Phi_{x,u-1,v} - M_{v-1}^- C_{v-1}^{v_2} \Phi_{x,u,v-1}]
 \end{aligned}$$

$$S_a^g = \tilde{S}^g$$

$$S_b^g = 0$$

$$S_a^h = \tilde{S}^h + \frac{\partial \langle U_2 U_3 \rangle}{\partial x_2} g$$

$$S_b^h = 0$$

$$S_a^j = \bar{S}^j + 2 \frac{\partial \langle U_2 U_3 \rangle}{\partial x_2} h + 2 \left( C_{f2} \varepsilon - \frac{C_p}{3} \frac{\partial \langle u_1 \rangle}{\partial x_2} \langle U_1 U_2 \rangle \right) g$$

$$S_b^j = -2C_{f1} \frac{\varepsilon}{k}$$

where,

$$\begin{aligned} C_{x+1}^{x_2} &= \frac{\bar{C}_{x+1/2}^{x_2}}{\delta(x_2)_{x+1/2}} & C_{x-1}^{x_2} &= \frac{\bar{C}_{x-1/2}^{x_2}}{\delta(x_2)_{x+1/2}} \\ C_{u+1}^{v_1} &= \frac{\bar{C}_{u+1/2}^{v_1}}{\delta(V_1)_{u+1/2}} & C_{u-1}^{v_1} &= \frac{\bar{C}_{u-1/2}^{v_1}}{\delta(V_1)_{u-1/2}} \\ C_{v+1}^{v_2} &= \frac{\bar{C}_{v+1/2}^{v_2}}{\delta(V_2)_{v+1/2}} & C_{v-1}^{v_2} &= \frac{\bar{C}_{v-1/2}^{v_2}}{\delta(V_2)_{v-1/2}} \\ D_{x+1}^{x_2} &= \frac{\bar{D}_{x+1/2}^{x_2}}{\delta(x_2)_{x+1} \delta(x_2)_{x+1/2}} & D_{x-1}^{x_2} &= \frac{\bar{D}_{x-1/2}^{x_2}}{\delta(x_2)_x \delta(x_2)_{x+1/2}} \\ D_{u+1}^{v_1} &= \frac{\bar{D}_{u+1/2}^{v_1}}{\delta(V_1)_{u+1} \delta(V_1)_{u+1/2}} & D_{u-1}^{v_1} &= \frac{\bar{D}_{u-1/2}^{v_1}}{\delta(V_1)_u \delta(V_1)_{u+1/2}} \\ D_{v+1}^{v_2} &= \frac{\bar{D}_{v+1/2}^{v_2}}{\delta(V_2)_{v+1} \delta(V_2)_{v+1/2}} & D_{v-1}^{v_2} &= \frac{\bar{D}_{v-1/2}^{v_2}}{\delta(V_2)_v \delta(V_2)_{v+1/2}} \end{aligned}$$

and

$$\delta(\cdot)_i = (\cdot)_i - (\cdot)_{i-1}$$

the bracket [ . . . ] denotes the function picking up the maximum of the values contained within it.

Since the Reynolds stress in mean velocity equation acts as a source term like mean pressure force, the staggered grid is needed to keep from a checkerboard solution.

## RESULTS AND DISCUSSION

In this section, the solution for  $g$ ,  $h$ , and  $j$  are discussed for the turbulent plane Couette flow. The physical properties of flow field are extracted from the three reduced distribution functions. Since the distribution functions are calculated by the finite difference method without making any assumption about the functional dependence on turbulence velocities, the distribution function can give an insight into the turbulence mechanism.

The solutions for  $h$  are nearly zero within the flow domain (which are within  $10^{-13}$  order compared with  $j$ ). From the definition of  $h$ , one can expect that the probability density function of  $V_3$ ,  $f(V_3)$ , is symmetric. We can find out this symmetric character for  $f(V_3)$  from Kreplin and Eckelmann's measurements<sup>34</sup>, *Figure 1*, which confirms the correctness of the present calculations.

*Figure 2* shows the mean velocity profiles computed in the present study and the experimental data of Reichardt<sup>20</sup> and Robertson *et al.*<sup>21</sup> The comparison of the present calculations with these experimental data shows a satisfactory agreement.

Results for Reynolds stress  $\langle U_1 U_2 \rangle$  normalized by square of frictional velocity are shown in *Figure 3*. The present results are in good agreement with the data of El Tebany *et al.*<sup>22</sup> since the Reynolds stress distribution determines the mean velocity profile of turbulent plane Couette flow, this agreement confirms the consistency of the calculations and the measurements.

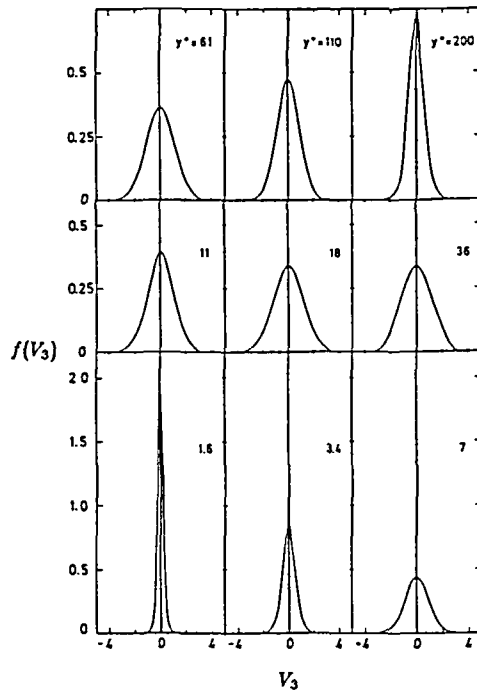


Figure 1 Probability density distributions of the velocity fluctuations,  $f(V_3)$ , measured by Kreplin and Eckelmann in turbulent channel flow

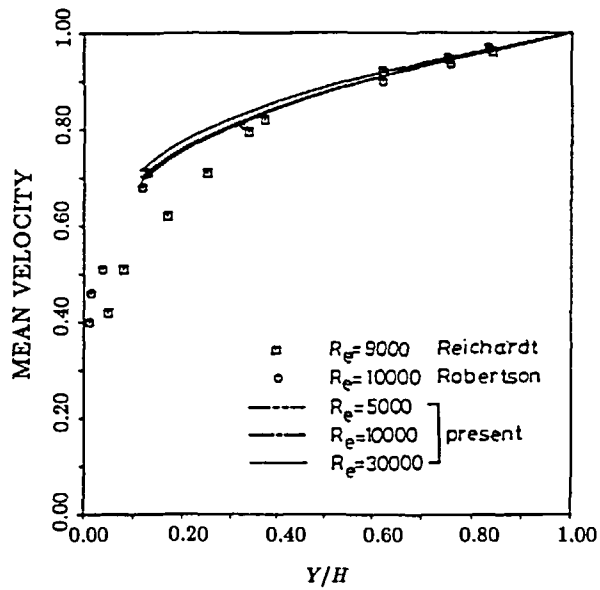


Figure 2 Mean velocity distributions

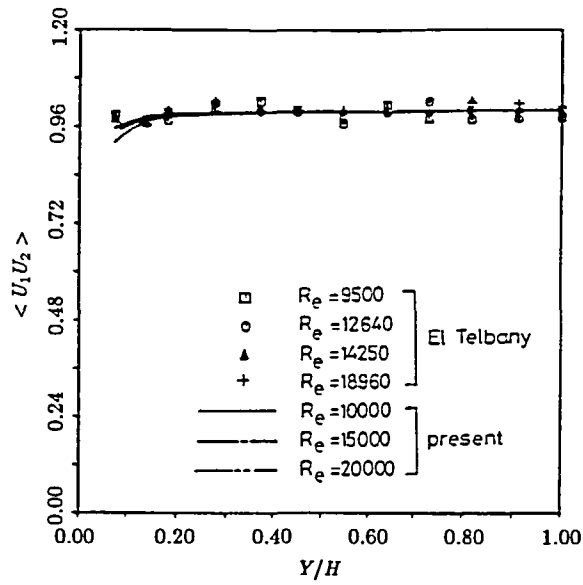


Figure 3 Reynolds stress distributions

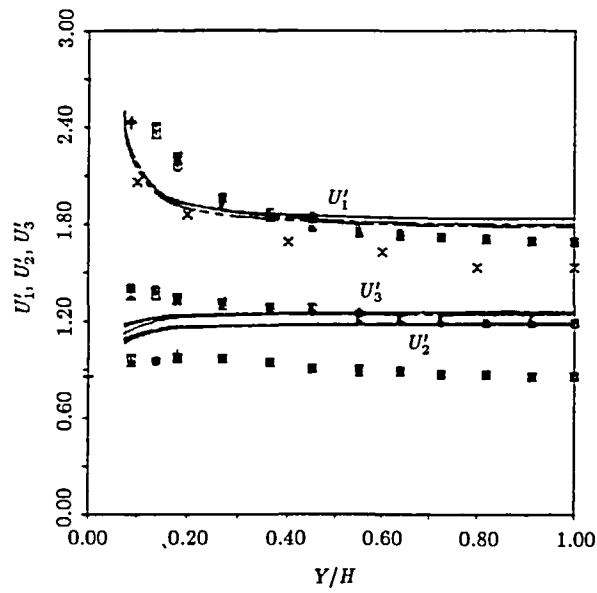
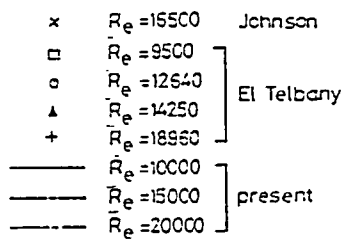


Figure 4 Turbulence intensity distributions





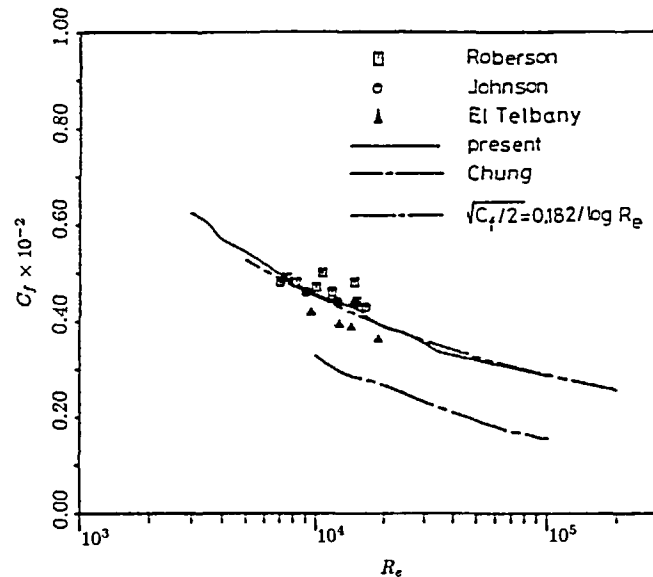


Figure 5 Dependence of the skin friction coefficient ( $C_f$ ) on the Reynolds number ( $Re$ )

The profiles of the three root mean squares of velocity fluctuations,  $\langle U_1 U_1 \rangle^{1/2}$ ,  $\langle U_2 U_2 \rangle^{1/2}$ , and  $\langle U_3 U_3 \rangle^{1/2}$ , normalized by frictional velocity are shown in Figure 4. Theoretically, the calculated values of  $\langle U_2 U_2 \rangle^{1/2}$  and  $\langle U_3 U_3 \rangle^{1/2}$  using the present pdf model shall be of the same values in Couette flow. In the present calculations,  $\langle U_2 U_2 \rangle^{1/2}$  and  $\langle U_3 U_3 \rangle^{1/2}$  are calculated from two different equations, i.e.  $g$  and  $j$ . The difference between  $\langle U_2 U_2 \rangle^{1/2}$  and  $\langle U_3 U_3 \rangle^{1/2}$  in Figure 4 is mainly due to the difference between the  $g$  and  $j$  difference equations. Nevertheless, it appears that the calculated values of the three rms velocity fluctuations are somewhat too large compared with experimental data of El Telbany *et al.*<sup>22</sup> and Johnson<sup>35</sup>.

Figure 5 illustrates the results for skin friction coefficient,  $C_f$ , compared with experimental data of Robertson<sup>21</sup>, Johnson<sup>35</sup>, and El Telbany *et al.*<sup>22</sup> Also Chung's results and Robertson's empirical expressions for predicting the skin friction coefficient are shown in this figure. The agreement between the present calculations and the empirical data is quite satisfactory.

The most interesting things in the present study are the shapes of distribution function. Since there are not any assumption about the functional dependence of distribution functions, they can reveal the turbulence intrinsic mechanisms. Figures 6 and 7 show the probability density function of  $V_1$  and  $V_2$ , respectively. The probability density of  $V_2$  have very little variation in the central core region, indicating that the boundary effects have slight influence on the velocity fluctuations normal to the wall, but more influence on the streamwise velocity fluctuations.

Figure 8 shows the isojoint probability density contours of  $V_1$  and  $V_2$ , while Figure 9 is the isojoint probability density contours for turbulent channel flow measured by Wallace and Brodkey<sup>36</sup>. The isojoint probability density contours in Figures 8 and 9 are very alike except the curves very near the central region. In channel flow the Reynolds stress tends to zero near the centre of the channel. Thus the isojoint probability density contour tends to an elliptic shape with  $V_1$  and  $V_2$  axis. In the present study, the Reynolds stress is constant in the central core of plane Couette flow. For symmetric requirement the isojoint probability density contour in the center of the two flat plate is elliptic with inclined major axes.

Figure 10 shows the isoline plots of the joint probability densities of  $V_1$  and  $V_2$  multiplied by  $V_1 V_2$ , i.e.  $V_1 V_2 \cdot g(V_1, V_2)$ . This value for each pair of  $V_1$  and  $V_2$  is a measure of the contribution

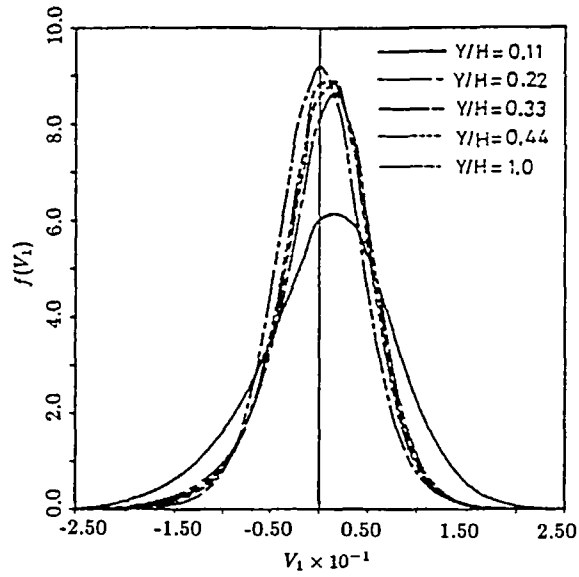


Figure 6 Probability density distributions of the streamwise velocity fluctuations,  $f(V_1)$

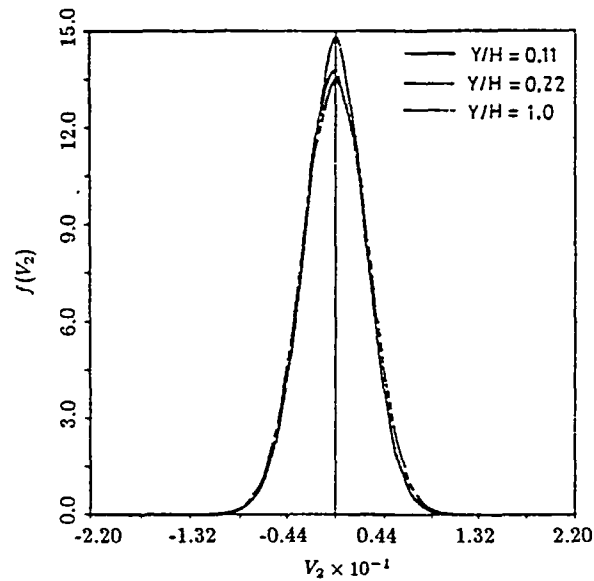


Figure 7 Probability density distributions of the velocity fluctuations normal to the wall  $f(V_2)$

of that pair of Reynolds stress. By definition,  $V_1 V_2 \cdot g(V_1, V_2)$  must be zero on each axis, and the distribution of contributions to Reynolds stress is split into four quadrants. Obviously, the larger contribution are seen in those quadrants associated with ejection and sweep motion in bursting phenomena.

Figure 11 shows the superimposed joint probability density distribution and the Reynolds

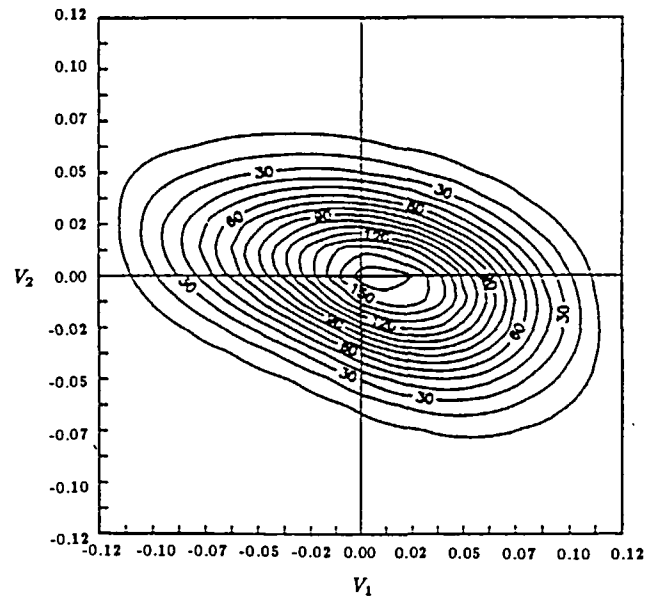


Figure 8a Isojoint probability density contours,  $f(V_1, V_2)$  at  $Y/H=0.11$  and  $Re=10^5$

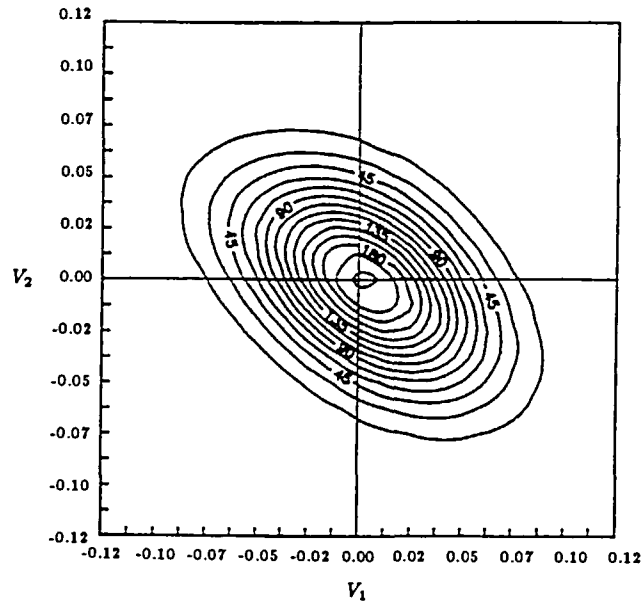


Figure 8b Isojoint probability density contours,  $f(V_1, V_2)$  at  $Y/H=0.56$  and  $Re=10^5$

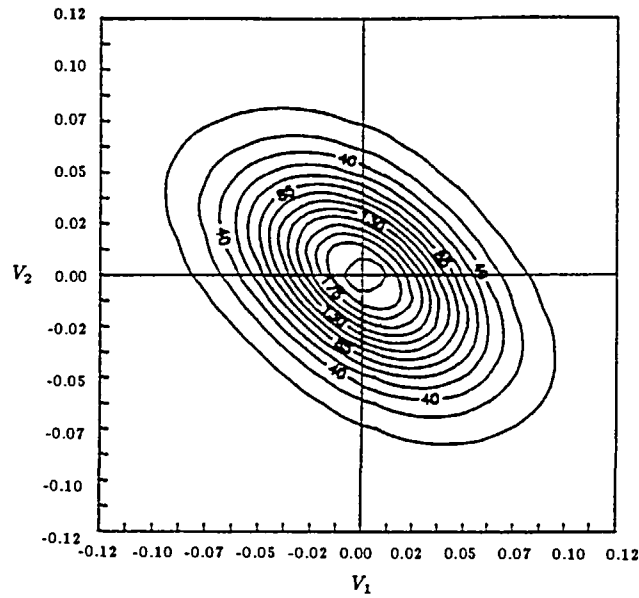


Figure 8c Isojoint probability density contours,  $f(V_1, V_2)$  at  $Y/H = 1.0$  and  $Re = 10^5$

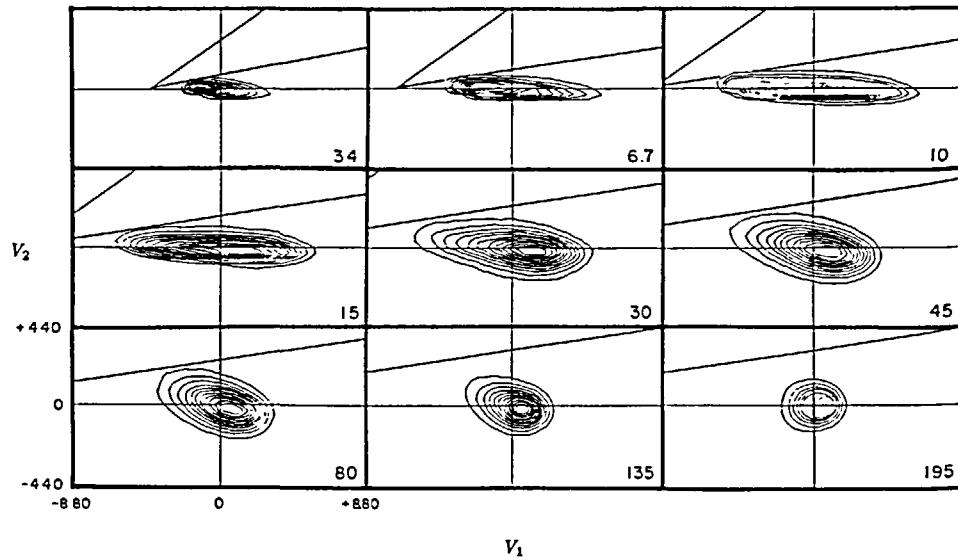


Figure 9 Isojoint probability density contours,  $f(V_1, V_2)$ , analyzed by Wallace and Brodkey in turbulent channel flow

stress contribution distributions at different  $Y/H$ . It clearly shows that the most probable pairs of velocities do not coincide with the pairs of velocities that give the largest contribution to the Reynolds stress. The energetic motions which are the principal source of Reynolds stress occur relatively seldom.

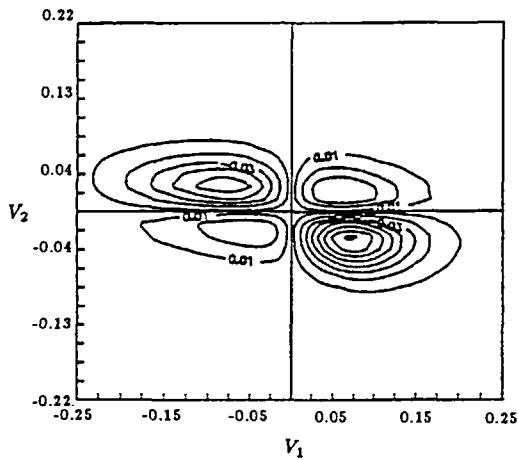


Figure 10a  $V_1V_2f(V_1, V_2)$  distributions of Couette flow at  $Y/H=0.11$  and  $Re=10^5$

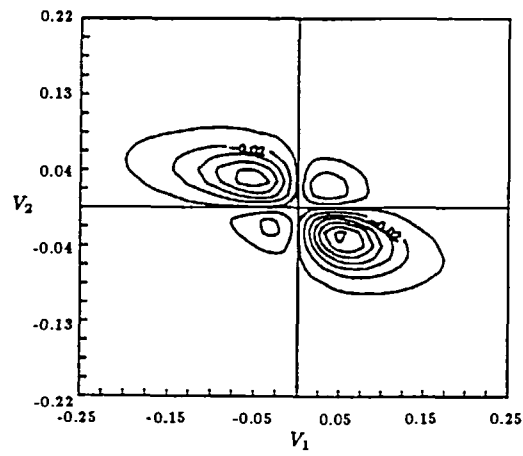


Figure 10b  $V_1V_2f(V_1, V_2)$  distributions of Couette flow at  $Y/H=0.56$  and  $Re=10^5$

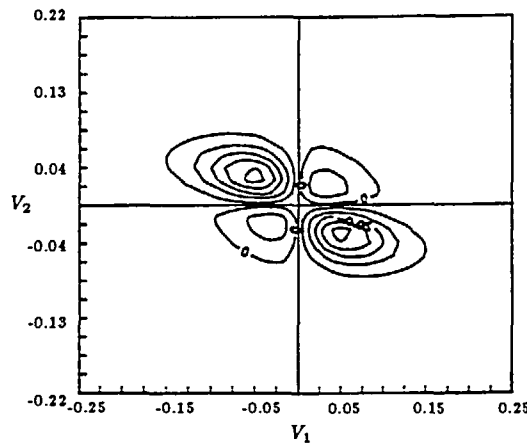


Figure 10c  $V_1V_2f(V_1, V_2)$  distributions of Couette flow at  $Y/H=1.0$  and  $Re=10^5$

CONCLUDING REMARKS

The pdf turbulent model developed earlier by the present authors have been solved with the finite difference method to calculate the one-point statistical properties of a turbulent plane Couette flow. For widely using first-order scheme such as upwind or hybrid scheme, the artificial diffusivity will cause some severe sources for turbulent energy. In order to avoid the artificial sources for turbulent energy a high order numerical scheme *QUICKER* was used to approach the first derivative terms of the velocity space.

As one knows that the physical properties change rapidly near solid wall in turbulent flow, a simple boundary treatment was proposed such that the boundary conditions can be directly set on the solid wall and no refined grid is needed.

The calculated mean velocity, Reynolds stress, and friction coefficient agree well with the available experimental data. The calculated isjoint probability density contours look very similar

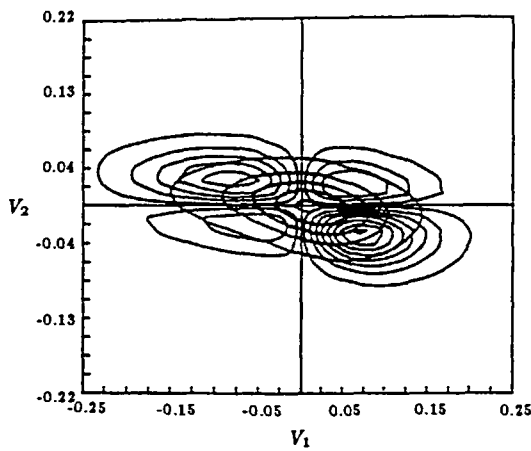


Figure 11a Superimposed  $f(V_1, V_2)$  distributions and  $V_1V_2f(V_1, V_2)$  distributions at  $Y/H=0.11$  and  $Re=10^5$

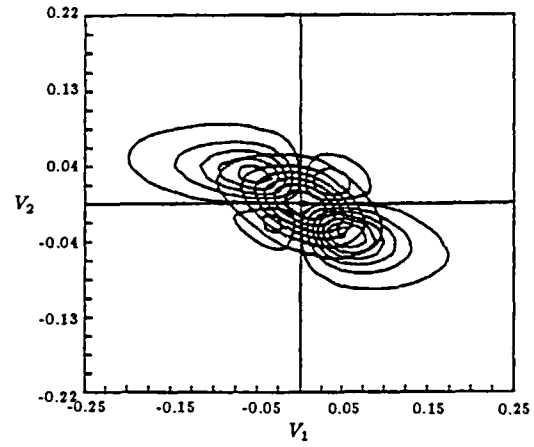


Figure 11b Superimposed  $f(V_1, V_2)$  distributions and  $V_1V_2f(V_1, V_2)$  distributions at  $Y/H=0.56$  and  $Re=10^5$

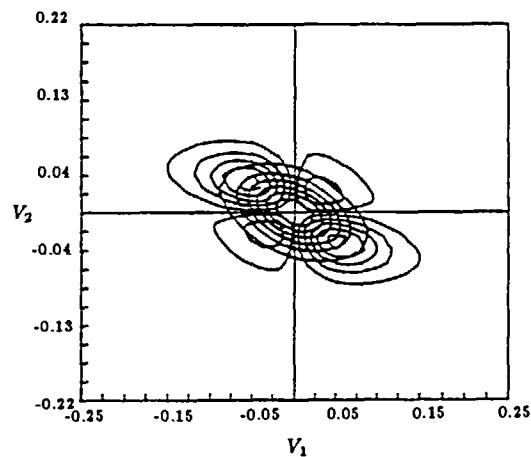


Figure 11c Superimposed  $f(V_1, V_2)$  distributions and  $V_1V_2f(V_1, V_2)$  distributions at  $Y/H=1.0$  and  $Re=10^5$

to experimental results. These agreements show that the new pdf model can satisfactorily describe the statistics of real turbulence and the near-wall treatment and *QUICKER* scheme do work in pdf model applications. Besides this result, the contribution of velocity pair to Reynolds stress and its relationship to the joint probability density function were also discussed. It shows that the pdf methods are of more potential in revealing turbulence structure than phenomenological turbulence models.

#### ACKNOWLEDGEMENTS

This research was partially supported by the National Science Council of the Republic of China under Contract NSC-78-0401-E008-09, which is herewith acknowledged.

## REFERENCES

- 1 Monin, A. S. Equation of turbulence motion, *Prikl. Mat. Mech.*, **31**, 1057–1065 (1967)
- 2 Hopf, E. Statistical hydrodynamics and functional calculus, *J. of Rational Mechanical Analysis*, **1**, 87–123 (1952)
- 3 Lundgren, T. S. Distribution function in the statistical theory of turbulence, *Phys. Fluids*, **10**, 969–975 (1967)
- 4 Lundgren, T. S. Model equation for non-homogeneous turbulence, *Phys. Fluids*, **12**, 485–497 (1969)
- 5 Pope, S. B. Transport equation for the joint probability density function of velocity and scalars in turbulence flow, *Phys. Fluids*, **A24**, 588–596 (1981)
- 6 Chung, P. M. A simplified statistical model of turbulent, chemically reacting shear flows, *AIAA J.*, **7**, 1982–1991 (1969)
- 7 Haworth, D. C. and Pope, S. B. A generalized Langevin model for turbulent flows, *Phys. Fluids*, **29**, 387–405 (1986)
- 8 Haworth, D. C. and Pope, S. B. A pdf modeling study of self-similar turbulent free shear flows, *Phys. Fluids*, **30**, 1026–1044 (1987)
- 9 Pope, S. B. A Lagrangian two-time probability density function equation for inhomogeneous turbulent flows, *Phys. Fluids*, **26**, 3448–3450 (1983)
- 10 Chung, P. M. On the development of diffusion flame in homologous turbulent shear flows, *AIAA Paper 70-722* (1970)
- 11 Hong, Z. C. and Lin, C. The turbulent kinetic equations characterized by three and many nonequilibrium degrees of freedom, *AIAA J.*, **28**, 1553–1554 (1990)
- 12 Lin, C. *Study on the Probability Density Function Models of Turbulent Flows*, Ph.D. Thesis, Department of Mechanical Engineering, National Taiwan University, Taiwan, R.O.C. (1989)
- 13 Hong, Z. C., Lin, C. and Chen, M. H. An Eulerian one-point velocity probability density function equation model for turbulent flows, *The Chinese J. of Mechanics*, **9**, 3, 167–179 (1993)
- 14 Chung, P. M. Turbulence description of Couette flow, *Phys. Fluids*, **16**, 980–987 (1973)
- 15 Srinivasan, R., Giddens, D. P., Bangert, L. H. and Wu, J. C. Turbulent plane Couette flow using probability distribution functions, *Phys. Fluids*, **20**, 557–567 (1977)
- 16 Bywater, R. J. Velocity space description of certain turbulent free shear flow characteristics, *AIAA J.*, **19**, 969–975 (1981)
- 17 Hong, Z. C. and Lai, Z. C. On the mixing analysis of a free turbulent shear layer, *The Chinese J. of Mechanics*, **1**, 25–33 (1983)
- 18 Pope, S. B. Calculations of a plane turbulent jet, *AIAA J.*, **22**, 896–904 (1984)
- 19 Pollard, A. and Siu, A. L.-W. The calculation of some laminar flows using various discretisation schemes, *Comput. Meths. Appl. Mech. Eng.*, **35**, 293–313 (1982)
- 20 Reichardt, V. H. Uber die geschwindigkeitsverteilung in einer geradlinigen turbulenten couettestromung, *Z. Angew. Math. Mech.*, **36**, 26 (1956)
- 21 Robertson, J. M. On turbulent plane Couette, *Proc. Sixth Midwestern Conf. Fluid-Mechanics* (Austin University Press, Austin, Texas), 169 (1959)
- 22 El Telbany, M. M. M. and Reynolds, A. J. The structure of turbulent plane Couette flow, *ASME J. Fluids Eng.*, **104**, 367 (1982)
- 23 Monin, A. S. and Yaglom, A. M. *Statistical Fluid Mechanics: Mechanics of Turbulence*, The MIT Press (1981)
- 24 Rotta, J. C. Statistische theorie nichthomogener turbulenz, *Zeitschrift fuer Physik*, **129**, 547–572 (1951)
- 25 Naot, D., Shavit, A. and Wolfshtein, M. Two-point correlation model and the redistribution of Reynolds stresses, *Phys. Fluids*, **16**, 738–743 (1973)
- 26 Mellor, G. and Herring, H. A survey of the mean turbulent field closure models, *AIAA J.*, **11**, 590–597 (1973)
- 27 Launder, B. E., Reece, G. J. and Rodi, W. Progress in the development of a Reynolds stress turbulence closure, *J. Fluid Mech.*, **68**, 537–566 (1975)
- 28 Noat, D., Shavit, A. and Wolfshtein, M. Interactions between components of the turbulent velocity correlation tensor, *Israel J. Tech.*, **8**, 259–265 (1970)
- 29 Reynolds, W. C. *Computation of Turbulent Flows-State-of-art*, Stanford University, Dept. Mech. Eng. Report MD-27 (1970)
- 30 Townsend, A. A. *The Structure of Turbulent Shear Flows*, Cambridge University Press, Cambridge (1956)
- 31 Anderson, D. A., Tannehill, J. C. and Pletcher, R. H. *Computational Fluid Mechanics and Heat Transfer*, Hemisphere Publishing Corporation, Washington (1984)
- 32 Patankar, S. V. *Numerical Heat Transfer and Fluid Flow*, Hemisphere Publishing Corporation, Washington (1980)
- 33 Leonard, B. P. A stable and accurate convective modelling procedure based on quadratic upstream interpolation, *Comput. Meths. Appl. Mech. Eng.*, **12**, 59–98 (1979)
- 34 Kreplin, H.-P. and Eckelmann, H. Behavior of the three fluctuating velocity components in the wall region of a turbulent channel flow, *Phys. Fluids*, **22**, 1233–1239 (1979)
- 35 Johnson, H. F. *An Experimental Study of Plane Couette flow*, M.S. Thesis, University of Illinois (1965)
- 36 Wallace, J. M. and Brodkey, R. S. Reynolds stress and joint probability density distributions in the U-V plane of a turbulent channel flow, *Phys. Fluids*, **20**, 351–355 (1977)